

Kinetics and Mechanism of Complex Formation of some Bivalent and Trivalent Metal Ions with Pentaammine-(nitrilotriacetato)cobalt(III) in Aqueous Medium†

Rita Das,^a Nigamananda Das^b and Anadi C. Dash^{*,c}

^a Department of Chemistry, M. P. C. College, Baripada-757 001, Orissa, India

^b Regional Research Laboratory, Bhubaneswar-751 013, Orissa, India

^c Department of Chemistry, Utkal University, Bhubaneswar-751 004, Orissa, India

The kinetics of reversible complex formation of Ni^{II}, Co^{II} and Cu^{II} with the pentaammine-(nitrilotriacetato)cobalt(III) ion, [Co(NH₃)₅(H₂nta)]²⁺ (H₃nta = nitrilotriacetic acid) have been investigated at 0.0025 ≤ [M²⁺] ≤ 0.04, 0.004 ≤ [H⁺] ≤ 0.05 mol dm⁻³, 10.0 ≤ T ≤ 40.0 °C and I = 0.3 mol dm⁻³. The rate constants for the formation of the binuclear species are at least 10³ times less than the water exchange rate constants of [M(OH₂)₆]²⁺ under comparable conditions. General base catalysis indicated that proton transfer from the NH⁺ site of the co-ordinated ligand (nta) is involved in the rate determining step. The binuclear species undergo dissociation *via* spontaneous and acid-catalysed paths. The low values of spontaneous dissociation rate constants also support the chelate nature of the binuclear species. It is likely that the nta moiety of (NH₃)₅Co(nta) acts at least as a tridentate ligand and the chelate ring closure/opening *via* N–Mⁿ bond formation/dissociation is rate limiting. Complex formation with Fe^{III} and Al^{III} has been investigated at 15–35 °C (I = 1.0 mol dm⁻³) and 25 °C (I = 0.3 mol dm⁻³), respectively. General base catalysis was not observed for these trivalent metal ions. The [M(OH₂)₅(OH)]²⁺ species reacted faster than [M(OH₂)₆]³⁺. The reaction of [M(OH₂)₆]³⁺ may involve an associative interchange mechanism while that for [M(OH₂)₅(OH)]²⁺ involves dissociative interchange.

The aquation of pentaammine(nitrilotriacetato)cobalt(III), [Co(NH₃)₅(H₂nta)]²⁺ (H₃nta = nitrilotriacetic acid), is reported¹ to be catalysed by metal ions *via* formation of reactive binuclear complexes. The kinetics and mechanism of formation/dissociation of binuclear species involving bivalent and trivalent metal ions and [Co(NH₃)₅(H₂nta)]²⁺ have not been reported. As a sequel to our current research interest on the study of the mechanism of formation/dissociation of binuclear complexes of metal ions with pentaammine-(carboxylato)cobalt(III) substrates^{2–9} we undertook the present study. The complex [Co(NH₃)₅(H₂nta)]²⁺ can exist in different stages of protonation under varying pH conditions resulting in species of varying charge with multiple co-ordinating sites. Thus the role of varying charge of the cobalt(III) substrate on the kinetics and mechanism of binuclear complex formation with some bivalent and trivalent metal ions could be examined. Further, the complexation kinetics of Cu^{II} is generally fast and requires the use of a relaxation technique to be followed. Interestingly the pentaammine(nitrilotriacetato)cobalt(III) cation proved suitable for the study of its complexation with Cu^{II} by a conventional stopped-flow technique.

Experimental

Materials and Methods.—Pentaammine(nitrilotriacetato)cobalt(III) perchlorate, [Co(NH₃)₅(H₂nta)][ClO₄]₂ [H₃nta = HN⁺(CH₂CO₂⁻)(CH₂CO₂H)₂] was prepared as described earlier.¹ The purity of the sample was checked by analysis of

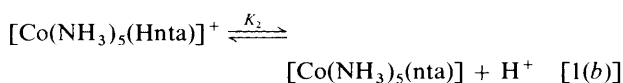
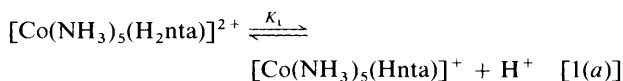
cobalt, and the UV/VIS spectral data of the complex agreed well with those reported earlier.¹ The FT-IR spectra of [Co(NH₃)₅(H₂nta)]²⁺ displayed bands at 1750 and 1632 cm⁻¹ attributed to free (ν_{CO₂H}) and cobalt(III)-bound carboxylate (ν_{CO₂M}) of the nta moiety, respectively.¹⁰ The latter band was broad presumably owing to the NH-deformation mode.

The stock solutions of Ni^{II}, Co^{II}, Cu^{II}, Al^{III} and Fe^{III} perchlorates were prepared and estimated as described earlier.¹¹ 2,6-Dimethylpyridine (Fluka, AG) was used whenever required. All other chemicals used for kinetic studies were of AR grade. Freshly prepared doubly distilled water was used in all experiments. The dissociation constants of the unbound carboxyl and protonated amine functions were determined potentiometrically at 15–35 °C, I = 0.3 and 1.0 mol dm⁻³. The pH measurements were made with an Elico digital model LI-120 pH-meter, using glass–Ag–AgCl, NaCl (2.0 mol dm⁻³) combined electrode model CL 51.

Kinetic Measurements.—The kinetics of reversible formation of binuclear complexes were studied under pseudo-first order conditions (5 < [M^{2+(3+)]/[complex]_T < 50) at suitable wavelengths (see footnotes to Tables 1, 5 and 6) using a fully automated Hi-Tech (UK) SF-51 stopped-flow spectrophotometer. For acid-catalysed dissociation the preformed binuclear complex was acidified rapidly in the stopped-flow assembly as described earlier.⁷ In every case absorbance–time data for any run fitted well to a single exponential equation applicable to first-order kinetics. At least seven replicate measurements were made for each run to compute *k*_{obs} and its standard deviation.}

Dissociation Constants.—The potentiometric titration using the method of Irving and Rossotti¹² yielded the acid dissociation constants [equation (1)] of the complex [p*K*₁ = 2.13 (2.05), 2.09 (1.96) and 2.03 (1.96); p*K*₂ = 8.20 (8.15),

† Supplementary data available (No. Sup 57104, 11 pp.): *k*_{obs} values at different temperatures. See Instructions for Authors, *J. Chem. Soc., Dalton Trans.*, 1995, Issue 1, pp. xxv–xxx.



7.91 (7.80) and 7.63 (7.55) at $I = 0.3$ (1.0) mol dm⁻³ and 15, 25 and 35 °C, respectively] in satisfactory agreement with those reported earlier [$\text{p}K_1 = 1.82 \pm 0.07$ (1.74 ± 0.2); $\text{p}K_2 = 7.96 \pm 0.01$ (8.3 ± 0.2) at 25 °C (6 °C) and $I = 1.0$ mol dm⁻³].¹

Results and Discussion

Reversible Formation of Binuclear Complexes Between Bivalent Metal Ions and [Co(NH₃)₅(H₂nta)]²⁺.—The interaction of the bivalent metal ions with [Co(NH₃)₅(H₂nta)]²⁺ is indicated by the instantaneous increase in absorbance in the range 260–320 nm (see Fig. 1). Our observations are in agreement with those of Cannon and Gardiner.¹ The pseudo-first-order rate constants [see equation (2)] were collected at varying [H⁺] (0.004–0.05 mol dm⁻³), [M²⁺] (0.005–0.04 for Co^{II} or Ni^{II} and 0.0025–0.020 for Cu^{II}) and are available as supplementary material (sup no. 57104). The plots of k_{obs} versus [M²⁺] are linear with positive intercepts on the rate axis; the slopes, however, increase with decreasing [H⁺]. This may be attributed to the reduced reactivity of [Co(NH₃)₅(H₂nta)]²⁺ relative to that of [Co(NH₃)₅(Hnta)]⁺. Plausible reaction pathways are given in Scheme 1. Accordingly k_{obs} takes the form given in equation (2), where the overall

$$k_{\text{obs}} = k_f[\text{M}^{2+}] + k_r \quad (2)$$

formation rate constant (k_f) and the dissociation rate constant (k_r) of the binuclear species, [(NH₃)₅Co(nta)M]²⁺, are given by equations (3) and (4), respectively. The k_f and k_r values are

$$k_f = \{k_1([\text{H}^+]/K_1) + k_2\}/(1 + [\text{H}^+]/K_1) \quad (3)$$

$$k_r = k_{-1}[\text{H}^+]^2 + k_{-2}[\text{H}^+] \quad (4)$$

obtained from the gradient and intercept of the least-squares best line plot of k_{obs} versus [M²⁺] at constant [H⁺]. The [H⁺] dependence of k_f enabled the calculation of k_1 and k_2 using equation (3) (see Table 1).

The [M(OH₂)₆]²⁺ (M²⁺ = Ni²⁺, Co²⁺ or Cu²⁺) ions are believed to undergo ligand substitution *via* a dissociative interchange mechanism (I_d).^{14–17} The complexation of these metal ions involves prior formation of the outer-sphere ion pair characterised by the equilibrium constant, K_{os} . The sequential displacement of three aqua ligands by the multidentate [Co(NH₃)₅(H₂nta)]²⁺ (=H₂L²⁺) may be delineated as in Scheme 2, where the substitution of any one of three aqua ligands may be rate determining. If substitution of the first aqua ligand in [M(OH₂)₆]²⁺ is rate determining then k_1' (= k_1/K_{os}) or k_2' (= k_2/K_{os}') should be comparable to the water exchange-rate constant of the aqua metal ions { $k_{\text{ex}} = 3.2 \times 10^4$, 3.2×10^6 and 4.4×10^9 s⁻¹ at 25 °C for [Ni(OH₂)₆]²⁺, [Co(OH₂)₆]²⁺ and [Cu(OH₂)₆]²⁺, respectively}.^{13,18} Using Fuoss's equation¹⁹ and assuming a distance of closest approach $a = 5 \text{ \AA}$ K_{os} was calculated to be 0.07 dm³ mol⁻¹ at 25 °C for a 2+–1+ charge outer-sphere interaction. An even lower value (≈0.05 dm³ mol⁻¹) of K_{os} is expected for 2+–2+ charge association. At 25 °C the values of k_1' {≈60, 1.2×10^3 and 2.3×10^5 s⁻¹} and k_2' {≈136, 3.0×10^3 and 7.1×10^5 s⁻¹, for Ni²⁺, Co²⁺ and Cu²⁺, respectively} estimated from K_{os} (K_{os}') are two to four orders of magnitude smaller than the water-exchange rate constants of Ni^{II}, Co^{II} and Cu^{II}. The rate constants for the formation of [(NH₃)₅Co(nta)M]²⁺ *via*

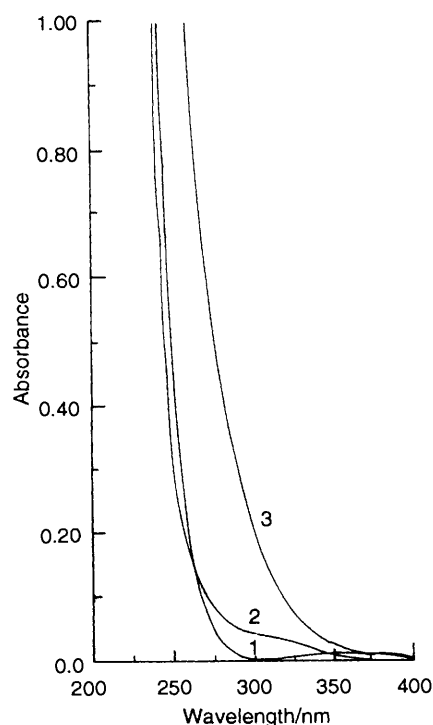
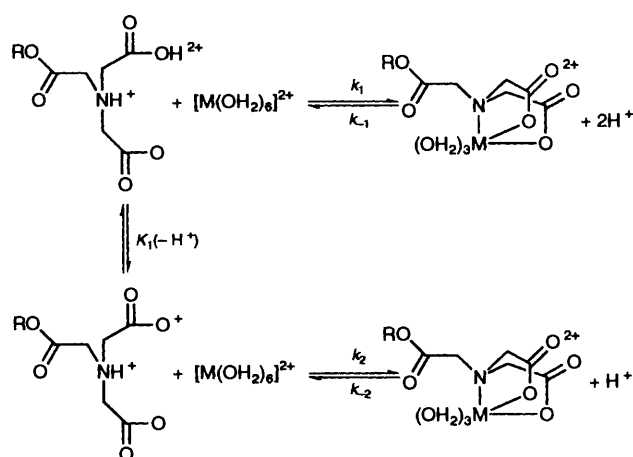
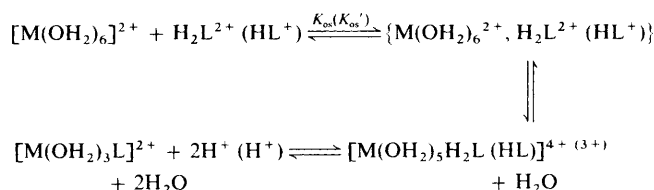


Fig. 1 Spectral evidence for the formation of binuclear complexes between [Co(NH₃)₅(H₂nta)]²⁺ and Cu²⁺ at [H⁺] = 1.0 × 10⁻², $I = 0.3$ mol dm⁻³: (1) [Cu²⁺] = 1.0 × 10⁻², (2) [complex]_T = 5.0 × 10⁻³ and (3) [Cu²⁺] = 1.0 × 10⁻², [complex]_T = 5.0 × 10⁻³ mol dm⁻³



Scheme 1 R = (NH₃)₅Co^{III}, M = Ni^{II}, Co^{II} or Cu^{II}



Scheme 2

the k_2 path are, however, comparable to the rate constants for the formation of [M(nta)]⁻ by the reaction of M²⁺ (M²⁺ = Ni²⁺ or Cu²⁺) with free Hnta²⁻ (see Table 2) reported earlier.^{20–23} This strongly suggests that the rate-determining step is not the loss of the first water molecule from the inner co-ordination sphere of the aqua metal ion. The relatively low rate constants for the formation of binuclear species, either by

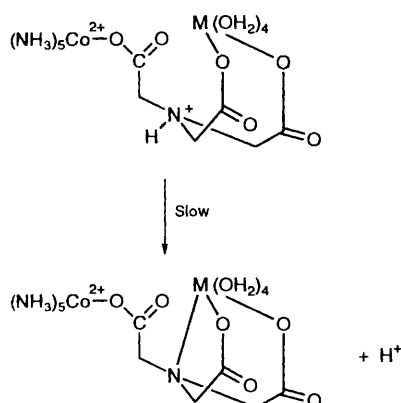
Table 1 Rate data and activation parameters for the formation of $[(\text{NH}_3)_5\text{Co}(\text{nta})\text{M}]^{2+ a}$

M	T/°C	$k_1/\text{dm}^3 \text{ mol}^{-1} \text{ s}^{-1}$	$k_2/\text{dm}^3 \text{ mol}^{-1} \text{ s}^{-1}$	$\Delta H^\ddagger/\text{kJ mol}^{-1}$	$\Delta S^\ddagger/\text{J K}^{-1} \text{ mol}^{-1 b}$
Ni ^{II}	20.0	2.9 ± 0.4	5.8 ± 0.3	62 ± 5 (49 ± 3)	-26 ± 15 (-63 ± 8)
	25.0	4.2 ± 0.4	6.8 ± 0.7		
	30.0	6.0 ± 0.2	10.5 ± 0.9		
	35.0	10.6 ± 0.6	17.7 ± 1.3		
	40.0	13.9 ± 0.5	21.7 ± 0.2		
Co ^{II}	15.0	31 ± 12	75 ± 7	83 ± 8 (52 ± 17)	70 ± 29 (-29 ± 57)
	20.0	46 ± 3	92 ± 4		
	25.0	84 ± 7	150 ± 9		
Cu ^{II}	10.0	(4.5 ± 0.4) × 10 ³	(15.2 ± 0.6) × 10 ³	62 ± 19 (38 ± 3)	51 ± 60 (-30 ± 6)
	15.0	(6.9 ± 1.0) × 10 ³	(18.8 ± 1.6) × 10 ³		
	20.0	(10.7 ± 1.0) × 10 ³	(27.4 ± 1.4) × 10 ³		
	25.0	(16.3 ± 0.6) × 10 ³	(35.9 ± 1.2) × 10 ³		

^a $[\text{Complex}]_T = (0.5\text{--}2.0) \times 10^{-3}$, $[\text{Ni}^{2+}]$ or $[\text{Co}^{2+}] = (0.5\text{--}5.0) \times 10^{-2}$, $[\text{Cu}^{2+}] = (0.25\text{--}2.0) \times 10^{-2}$, $I = 0.3 \text{ mol dm}^{-3}$, $\lambda = 260$ for Ni²⁺ and Co²⁺ and 290 nm for Cu²⁺. ^b Values for k_2 (k_1 values in parentheses); $\Delta H_{\text{ex}}^\ddagger/\text{kJ mol}^{-1}$ ($\Delta S_{\text{ex}}^\ddagger/\text{J K}^{-1} \text{ mol}^{-1}$) = 57 (32) and 47 (37) for the H₂O exchange reaction of $[\text{Ni}(\text{OH}_2)_6]^{2+}$ and $[\text{Co}(\text{H}_2\text{O})_6]^{2+}$ respectively (ref. 13).

Table 2 Comparison of rate parameters for the formation of bivalent metal complexes with free and partially co-ordinated nitrilotriacetate at 25 °C

Reaction	$I/\text{mol dm}^{-3}$	$k_r/\text{dm}^3 \text{ mol}^{-1} \text{ s}^{-1}$	Refs.
Ni ²⁺ + Hnta ²⁻	1.25	7.51	20
	0.20	4.0	21
Ni ²⁺ + $[\text{Co}(\text{NH}_3)_5(\text{Hnta})]^+$	0.30	6.8 ± 0.7	This work
	—	5.0 × 10 ³	22
Cu ²⁺ + Hnta ²⁻	0.05	1.12 × 10 ⁵	23
	0.30	(36 ± 1) × 10 ³	This work
Co ²⁺ + $[\text{Co}(\text{NH}_3)_5(\text{Hnta})]^+$	0.30	150 ± 9	This work

**Scheme 3** M²⁺ = Ni²⁺, Co²⁺ or Cu²⁺

path k_1 or k_2 , indicate that chelate-ring formation through N (see Scheme 3) is rate limiting. A similar interpretation has been made in studies of a number of metal aminopolycarboxylic acid complexes.^{20–26} If so, then either the proton migrates from the N atom to the solvent before chelate-ring closure, or proton transfer from the NH⁺ site and chelate-ring closure are acting in concert. Additional evidence of rate-limiting proton transfer from the NH⁺ centre is obtained from buffer catalysis, *i.e.* k_{obs} at a fixed pH and $[\text{Ni}^{2+}]$ is found to increase with increasing 2,6-dimethylpyridine concentration (see Table 3). The activation parameters (ΔH^\ddagger and ΔS^\ddagger) are also substantially different from those reported for the water-exchange reaction of $[\text{M}(\text{OH}_2)_6]^{2+}$ ions (see Table 1) { $\Delta H^\ddagger = 57, 47$ and 17 kJ mol^{-1} ; $\Delta S^\ddagger = 32, 37$ and $-44 \text{ J K}^{-1} \text{ mol}^{-1}$ for $[\text{Ni}(\text{OH}_2)_6]^{2+}$, $[\text{Co}(\text{OH}_2)_6]^{2+}$ and $[\text{Cu}(\text{MeOH})_6]^{2+}$, respectively}.¹³

Rate data for the acid-catalysed dissociation of binuclear complexes, $[(\text{NH}_3)_5\text{Co}(\text{nta})\text{M}]^{2+}$ at various temperatures and $[\text{H}^+]$ ($I = 0.3 \text{ mol dm}^{-3}$) are available as supplementary data. The observed rate constants were corrected for the formation reaction by utilising the values of k_1 , k_2 and K_1 . The plots of the corrected pseudo-first-order rate constant, $k_r (=k_{\text{obs}} -$

Table 3 Effect of 2,6-dimethylpyridine concentration on the rate of formation of $[(\text{NH}_3)_5\text{Co}(\text{nta})\text{Ni}]^{2+}$ at 25 °C*

$[\text{C}_5\text{H}_3\text{Me}_2\text{N}]/\text{mol dm}^{-3}$	$[\text{HClO}_4]/\text{mol dm}^{-3}$	pH	$k_{\text{obs}}/\text{s}^{-1}$
0.01	0.005	6.72	60 ± 4
0.02	0.010	6.73	70 ± 4
0.03	0.015	6.74	75 ± 7
0.04	0.020	6.72	80 ± 7
0.05	0.025	6.77	85 ± 9
0.06	0.030	6.76	90 ± 8

* $[\text{Complex}]_T = 1.0 \times 10^{-3}$, $[\text{Ni}^{2+}] = 2.0 \times 10^{-2}$, $I = 0.3 \text{ mol dm}^{-3}$; $\lambda = 290 \text{ nm}$.

$k_r[\text{Ni}^{2+}]$ versus $[\text{H}^+]$ are not linear; however, the plots of $k_r/[\text{H}^+]$ versus $[\text{H}^+]$ yielded good straight lines, consistent with equation (4) (see Fig. 2). The values of k_{-1} and k_{-2} obtained from the slopes and intercepts of such plots and their associated activation parameters are collected in Table 4.

A comparison of the dissociation rate constants, k_{-2} , for $[(\text{NH}_3)_5\text{Co}(\text{nta})\text{Ni}]^{2+}$ (5.0) and $[\text{Ni}(\text{nta})]^-$ ($0.77 \text{ dm}^3 \text{ mol}^{-1} \text{ s}^{-1}$ at 25 °C, $I = 0.3$ and 1.0 mol dm^{-3})²⁰ showed that the former is only six times kinetically more labile than the latter. Analogous rate comparisons for Co²⁺ and Cu²⁺ cannot be made due to non-availability of rate data for the acid-catalysed dissociation of $[\text{Co}(\text{nta})]^-$ and $[\text{Cu}(\text{nta})]^-$. However, the small rate difference for Ni²⁺ indicates that the M²⁺ ions are chelated by the nta moiety in $[(\text{NH}_3)_5\text{Co}(\text{nta})\text{M}]^{2+}$, H⁺-promoted Ni–N bond cleavage being the most likely rate-determining step. Indeed, Bydalek and Blomster²⁰ have suggested that Ni–N bond cleavage is rate determining in the dissociation of $[\text{Ni}(\text{nta})]^-$.

Reversible Formation of Binuclear Complexes of M³⁺ Ions with $[\text{Co}(\text{NH}_3)_5(\text{H}_2\text{nta})]^{2+}$.—The observed pseudo-first-order rate constants for the formation of Fe³⁺ are available as supplementary material while those of Al³⁺ are presented in Table 5. Plots of k_{obs} versus $[\text{M}^{3+}]$ at fixed $[\text{H}^+]$ are linear with positive intercepts and gradients which are identified with the overall dissociation and formation rate constants of the

binuclear species, respectively. Scheme 4 delineates the overall reaction sequence for which k_{obs} is given by equation (5) where

$$k_{\text{obs}} = k_f f_1 f_2 [\text{M}^{3+}] + k_r \quad (5)$$

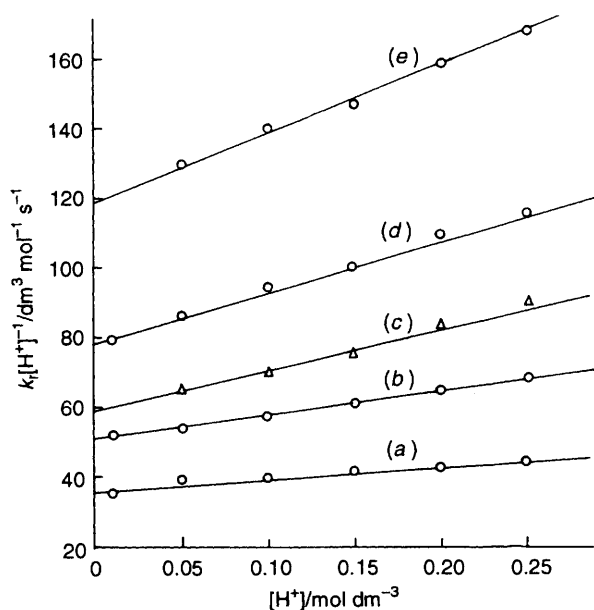


Fig. 2 Plots of $k_f/[\text{H}^+]$ ($k_r = k_{\text{obs}} - k_f[\text{Ni}^{2+}]$) versus $[\text{H}^+]$ for the acid-catalysed dissociation of $[(\text{NH}_3)_5\text{Co}(\text{nta})\text{Ni}]^{2+}$ at 20 (a), 25 (b), 30 (c), 35 (d) and 40 °C (e)

k_f , k_r , f_1 and f_2 are defined as in equations (6)–(9). Values of K_h

$$k_f = k_1 + (k_2 K_h + k_3 K_1)/[\text{H}^+] + k_4 K_1 K_h/[\text{H}^+]^2 \quad (6)$$

$$k_r = k_{-4} + (k_{-2} + k_{-3})[\text{H}^+] + k_{-1}[\text{H}^+]^2 \quad (7)$$

$$f_1 = [\text{H}^+]/([\text{H}^+] + K_h) \quad (8)$$

$$f_2 = [\text{H}^+]/([\text{H}^+] + K_1) \quad (9)$$

for $[\text{Fe}(\text{OH}_2)_6]^{3+}$ $[(1.2\text{--}2.3) \times 10^{-3} \text{ mol dm}^{-3}$ at 20–35 °C, $I = 1.0 \text{ mol dm}^{-3}]^{27}$ and of K_1 (see Experimental section) are such that f_1 and f_2 reduce virtually to unity in the experimental acidity range so that equation (5) reduces to equation (10).

$$k_{\text{obs}} = k_f[\text{Fe}^{3+}] + k_r \quad (10)$$

However, for Al^{3+} , $f_1 = 1$ and f_2 is significantly less than 1 in the acidity range employed $\{K_h \text{ of } [\text{Al}(\text{OH}_2)_6]^{3+} = 1.0 \times 10^{-5} \text{ mol dm}^{-3}$ at 25 °C, $I = 0.1 \text{ mol dm}^{-3}\}^{28}$ and hence equation (5) reduces to equation (11). Linear plots of k_{obs} versus $[\text{Fe}^{3+}]$ or

$$k_{\text{obs}} = k_f[\text{Al}^{3+}]\{[\text{H}^+]/([\text{H}^+] + K_1)\} + k_r \quad (11)$$

$[\text{Al}^{3+}]/f_2$ yielded k_f and k_r values as the slopes and intercepts, respectively and good linear plots of $k_f/[\text{H}^+]$ against $[\text{H}^+]^{-1}$ (Fig. 3) were also obtained. Hence k_1 is insignificant, *i.e.*, the dipositive form of the complex, $[\text{Co}(\text{NH}_3)_5(\text{H}_2\text{nta})]^{2+}$ does not react with $[\text{M}(\text{OH}_2)_6]^{3+}$. A similar observation was made in the complexation reaction of Fe^{3+} with pentaammine(oxalato)cobalt(III).² The values of $k_4 K_h K_1$ (and k_4) and $(k_2 K_h + k_3 K_1)$ calculated from the gradients and intercepts of $k_f/[\text{H}^+]$ versus $[\text{H}^+]^{-1}$ plots are collected in Table 6. The values of k_2

Table 4 Rate and activation parameters for the dissociation of $[(\text{NH}_3)_5\text{Co}(\text{nta})\text{M}]^{2+}$ ^a

M	T/°C	$k_{-1}/\text{dm}^6 \text{ mol}^{-2} \text{ s}^{-1}$	$k_{-2}/\text{dm}^3 \text{ mol}^{-1} \text{ s}^{-1}$	$\Delta H^\ddagger/\text{kJ mol}^{-1}$	$\Delta S^\ddagger/\text{J K}^{-1} \text{ mol}^{-1}$
Ni ^{II}	20.0	3.5 ± 0.5	3.6 ± 0.1	45 ± 8 (45 ± 5)	80 ± 28 (-80 ± 16)
	25.0	8.0 ± 0.3	5.0 ± 0.1		
	30.0	14.1 ± 1.0	5.6 ± 0.2		
	35.0	15.2 ± 0.7	7.8 ± 0.1		
	40.0	18.8 ± 0.9	12.2 ± 0.1		
Co ^{II}	15.0	$(3.0 \pm 0.2) \times 10^2$	$(3.9 \pm 0.1) \times 10^2$	79 ± 10 (55 ± 6)	76 ± 36 (-14 ± 18)
	20.0	$(6.0 \pm 0.4) \times 10^2$	$(6.9 \pm 0.1) \times 10^2$		
	25.0	$(9.2 \pm 0.7) \times 10^2$	$(9.4 \pm 0.1) \times 10^2$		
Cu ^{II}	10.0	$(12.5 \pm 0.1) \times 10^2$	$(2.3 \pm 0.3) \times 10^2$	40 ± 2 (18 ± 8)	-41 ± 6 (-137 ± 27)
	15.0	$(16.5 \pm 1.4) \times 10^2$	$(3.2 \pm 0.3) \times 10^2$		
	20.0	$(24.0 \pm 0.6) \times 10^2$	$(3.6 \pm 0.1) \times 10^2$		
	25.0	$(29.7 \pm 1.5) \times 10^2$	$(3.7 \pm 0.3) \times 10^2$		

^a $[\text{Complex}]_T = (0.5\text{--}1.0) \times 10^{-3}$, $[\text{M}^{2+}] = (0.5\text{--}1.0) \times 10^{-2}$, $I = 0.3 \text{ mol dm}^{-3}$; $\lambda = 260$ for Ni^{2+} and Co^{2+} and 290 nm for Cu^{2+} . ^b Values evaluated from dependence of temperature on k_{-1} (k_{-2}).

Table 5 Rate data for the formation of $[(\text{NH}_3)_5\text{Co}(\text{nta})\text{Al}]^{3+}$ at 25 °C ^a

$10^2 [\text{Al}^{3+}]/\text{mol dm}^{-3}$	$10^3 k_{\text{obs}}/\text{s}^{-1}$ ^b			
	$(2.55 \pm 0.02)^b$	(2.70 ± 0.02)	(2.85 ± 0.03)	(3.05 ± 0.02)
0.50	12.0 ± 0.2	14.1 ± 0.8	16.0 ± 0.7	17.2 ± 1.9
1.00	13.5 ± 0.6	15.8 ± 0.8	18.5 ± 0.4	21.2 ± 1.1
1.50	14.2 ± 0.3	17.4 ± 0.5	20.7 ± 1.4	25.6 ± 1.4
2.00	15.6 ± 0.1	19.0 ± 0.8	23.1 ± 0.6	27.8 ± 1.6
2.50	17.2 ± 0.8	19.8 ± 0.6	25.6 ± 0.4	31.7 ± 1.6
3.00	17.6 ± 0.2	21.0 ± 0.6	29.0 ± 1.2	35.0 ± 0.5
4.00	19.9 ± 0.6	25.0 ± 0.6	—	—
$k_f/\text{dm}^3 \text{ mol}^{-1} \text{ s}^{-1}$	0.71 ± 0.02	1.15 ± 0.05	2.45 ± 0.07	5.2 ± 0.1
$10^3 k_r/\text{s}^{-1}$	10.9 ± 0.1	12.6 ± 0.4	13.6 ± 0.3	14.0 ± 0.4

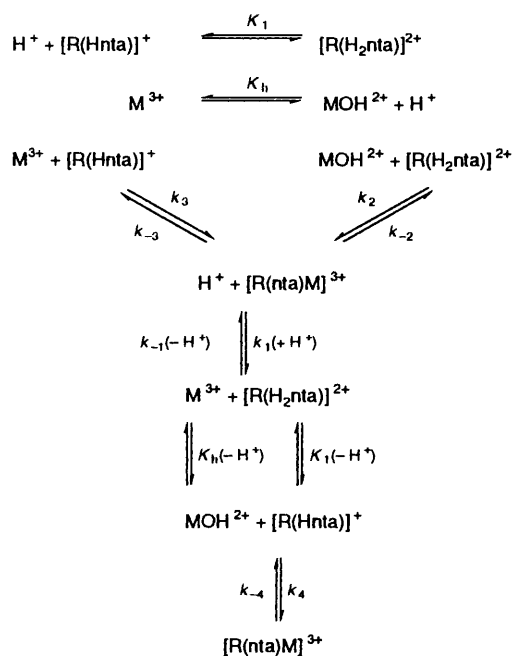
$k_4 = 85 \pm 10 \text{ dm}^3 \text{ mol}^{-1} \text{ s}^{-1}$ $10^3 (k_2 K_h + k_3 K_1) = 1.0 \pm 0.3 \text{ s}^{-1}$ $k_2 = 48 \text{ dm}^3 \text{ mol}^{-1} \text{ s}^{-1}$ $10^2 k_3 = 6.2 \text{ dm}^3 \text{ mol}^{-1} \text{ s}^{-1}$

^a $[\text{Complex}]_T = 1.0 \times 10^{-3}$, $I = 0.3 \text{ mol dm}^{-3}$, $\lambda = 270 \text{ nm}$. ^b Values in parentheses denote pH.

Table 6 Rate and activation parameters for the formation of $[(\text{NH}_3)_5\text{Co}(\text{nta})\text{Fe}]^{3+}$ ^a

<i>T</i> /(°C)	$10^2 [\text{H}^+]/\text{mol dm}^{-3}$	$k_t/\text{dm}^3 \text{ mol}^{-1} \text{ s}^{-1}$	$10^2 (k_2K_h + k_3K_1)/\text{s}^{-1}$	$10^{-3} k_4/\text{dm}^3 \text{ mol}^{-1} \text{ s}^{-1}$	$10^{-2} k_2/\text{dm}^3 \text{ mol}^{-1} \text{ s}^{-1}$	$k_3/\text{dm}^3 \text{ mol}^{-1} \text{ s}^{-1}$	$k_t(\text{av.})^b/\text{s}^{-1}$
15.0	5.0	21.1 ± 0.5	43 ± 3	2.7 ± 0.3	2.4	24	0.06 ± 0.02
	10.0	8.0 ± 0.5					
	15.0	5.3 ± 0.3					
20.0	20.0	3.7 ± 0.4	85 ± 10	5.4 ± 1.0	3.5	42	0.11 ± 0.03
	5.0	43 ± 3					
	10.0	14.5 ± 1.2					
	15.0	8.8 ± 0.3					
25.0	20.0	5.2 ± 0.6	186 ± 17	6.2 ± 1.2	5.7	85	0.19 ± 0.08
	5.0	75 ± 4					
	10.0	30.0 ± 1.2					
	15.0	16.7 ± 0.7					
35.0	20.0	10.9 ± 0.3	594 ± 19	8.0 ± 0.4	10	266	0.56 ± 0.21
	5.0	223 ± 8					
	10.0	88 ± 5					
	15.0	51 ± 2					
	20.0	36 ± 2					
$\Delta H^\ddagger/\text{kJ mol}^{-1}$				34 ± 7	48 ± 4	87 ± 2	
$\Delta S^\ddagger/\text{J K}^{-1} \text{ mol}^{-1}$				-61 ± 22	-33 ± 13	82 ± 6	

^a $[\text{Complex}]_T = 1.0 \times 10^{-3}$, $I = 1.0 \text{ mol dm}^{-3}$; $\lambda = 400 \text{ nm}$. ^b From average values of the intercepts of k_{obs} vs. $[\text{Fe}^{3+}]_T$ plots at different acidities [see equation (10)].



Scheme 4 R = $(\text{NH}_3)_5\text{Co}^{3+}$, nta = $\text{N}(\text{CH}_2\text{CO}_2)_2$, $\text{M}^{3+} = \text{Fe}^{3+}$ or Al^{3+}

and k_3 could not be determined accurately but have been estimated as follows. It is reasonable to assume that $k_{-2} = k_{-3}$, since the transition states for these dissociation paths should not differ greatly. Any difference in the distribution of hydrolysis products of the binuclear species is expected to arise, at a given acidity, by very rapid proton transfers governed by K_1 and K_h . Considering the interrelationships of the various equilibria in Scheme 4 the assumption $k_2K_h/k_3K_1 = k_{-2}/k_{-3}$, can be made for which $k_2K_h = k_3K_1$. Thus, the values of k_2 and k_3 are estimated. The various rate parameters for Fe^{III} complexation are collected in Table 6, with the corresponding rate parameters for Al^{III} in Table 5.

The kinetic results for the formation of Fe^{III} complexes with some related carboxylate and aminocarboxylate ligands are summarised in Table 7. It is interesting that the formation rate constants by various pathways in the nta system are comparable (within a factor of 10) with analogous rate

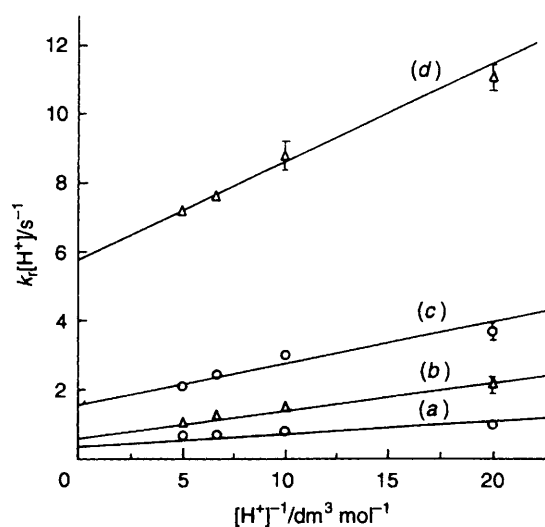


Fig. 3 Plots of $k_t[\text{H}^+]$ versus $[\text{H}^+]^{-1}$ for the formation of $[(\text{NH}_3)_5\text{Co}(\text{nta})\text{Fe}]^{3+}$ at 15 (a), 20 (b), 25 (c) and 35 °C (d)

constants for other carboxylate systems.^{2,6,29-35} Assuming an I_d mechanism and using $k = k^*K_{\text{os}}$,³⁶ where K_{os} is the outer-sphere association constant as defined earlier and k^* is the water-exchange rate constant for the ion pair, the values of k^* for Fe^{3+} or FeOH^{2+} complexation with various 0 and -1 charged ligands ($K_{\text{os}} = 0.15\text{--}2.1 \text{ mol dm}^{-3}$) can be calculated; and fall in the ranges $1.2\text{--}1500 \text{ s}^{-1}$ and $(0.1\text{--}5.0) \times 10^4 \text{ s}^{-1}$, respectively.^{37,38} The value of K_{os} for Fe^{3+} or FeOH^{2+} with neutral ligands is reported³⁹ to be $0.3 \text{ dm}^3 \text{ mol}^{-1}$ at 25 °C ($I = 1.0 \text{ mol dm}^{-3}$). Even lower values of K_{os} are expected for $3+-2+$, $2+-2+$ and $2+-1+$ charge associations. A value of $K_{\text{os}} = 0.07 \text{ dm}^3 \text{ mol}^{-1}$ for $2+-1+$ charge association (as estimated for bivalent metal ions, 25 °C, $I = 0.3 \text{ mol dm}^{-3}$) yielded $k_4^* = 0.88 \times 10^5 \text{ s}^{-1}$ (at 25 °C). This is close to the value of the water-exchange rate constant of FeOH^{2+} ($1.4 \times 10^5 \text{ s}^{-1}$).^{37,40} By an identical calculation, using $K_{\text{os}} \approx 0.05 \text{ dm}^3 \text{ mol}^{-1}$ for $3+-1+$ and $2+-2+$ associations, k_2^* and k_3^* were found to be $\approx 1.13 \times 10^4 \text{ s}^{-1}$ and $\approx 1.7 \times 10^3 \text{ s}^{-1}$ (25 °C, $I = 1.0 \text{ mol dm}^{-3}$), respectively. Comparison of these values with the water-exchange rate constants of $[\text{Fe}(\text{OH}_2)_6]^{3+}$ and $[\text{Fe}(\text{OH}_2)_5\text{OH}]^{2+}$ [$k_{\text{ex}}(\text{Fe}^{3+}) = 1.6 \times 10^2 \text{ s}^{-1}$,

Table 7 Comparison of rate parameters for the formation of Fe^{III} complexes with some carboxylate ligands at 25 °C: 0.5 ≤ pH ≤ 2.5*

Reacting species	$I/\text{mol dm}^{-3}$	$k/\text{dm}^3 \text{ mol}^{-1} \text{ s}^{-1}$	Ref.
$\text{Fe}^{3+} + [\text{Co}(\text{NH}_3)_5(\text{C}_2\text{O}_4)]^+$	1.0	870	2
$\text{FeOH}^{2+} + [\text{Co}(\text{NH}_3)_5(\text{C}_2\text{O}_4)]^+$	1.0	3.7×10^4	2
$\text{FeOH}^{2+} + [\text{Co}(\text{NH}_3)_5(\text{HC}_2\text{O}_4)]^{2+}$	1.0	4.6×10^3	2
$\text{FeOH}^{2+} + [\text{Co}(\text{NH}_3)_5(\text{Hmal})]^{2+}$	0.5	1.26×10^4	6
$\text{Fe}^{3+} + [\text{Co}(\text{NH}_3)_5(\text{Hmal})]^{2+}$	0.5	71	6
$\text{Fe}^{3+} + [\text{Co}(\text{NH}_3)_5(\text{Hnta})]^+$	1.0	85	This work
$\text{FeOH}^{2+} + [\text{Co}(\text{NH}_3)_5(\text{H}_2\text{nta})]^{2+}$	1.0	5.7×10^2	This work
$\text{FeOH}^{2+} + [\text{Co}(\text{NH}_3)_5(\text{Hnta})]^+$	1.0	6.2×10^3	This work
$\text{FeOH}^{2+} + \text{H}_2\text{nta}^-$	0.5	1.0×10^5	29
		5.6×10^4	30
$\text{FeOH}^{2+} + \text{H}_3\text{nta}$	0.5	1.5×10^4	29
$\text{FeOH}^{2+} + \text{H}_2\text{ida}$	—	2.5×10^3	29
$\text{FeOH}^{2+} + \text{Hida}^-$	—	8.8×10^3	29
$\text{FeOH}^{2+} + \text{MeCO}_2\text{H}$	0.5	2.8×10^3	31
$\text{Fe}^{3+} + \text{MeCO}_2\text{H}$	0.5	27	31
$\text{FeOH}^{2+} + \text{CH}_2\text{ClCO}_2\text{H}$	1.0	8.3×10^3	32
$\text{Fe}^{3+} + \text{HC}_2\text{O}_4^-$	1.0	8.6×10^2	33
$\text{FeOH}^{2+} + \text{HC}_2\text{O}_4^-$	1.0	2.0×10^4	33
$\text{Fe}^{3+} + \text{H}_2\text{pydca}$	1.0	34	34
$\text{FeOH}^{2+} + \text{H}_2\text{pydca}$	1.0	1.5×10^4	34
$\text{Fe}^{3+} + \text{H}_3\text{L}^{1+}$	0.1	180	35
$\text{FeOH}^{2+} + \text{H}_3\text{L}^{1+}$	0.1	1.27×10^3	35
$\text{Fe}^{3+} + \text{H}_3\text{L}^{2+}$	0.1	108	35
$\text{FeOH}^{2+} + \text{H}_3\text{L}^{2+}$	0.1	5.28×10^3	35
$\text{Fe}^{3+} + \text{H}_3\text{L}^3$	0.1	52	35
$\text{FeOH}^{2+} + \text{H}_4\text{L}^{3+}$	0.1	1.31×10^3	35

* H₂mal = malonic acid, H₂ida = iminodiacetic acid, H₂pydca = pyridine-2,6-dicarboxylic acid, H₂L¹ = R-L-Phe, H₂L² = R-L-Ala, H₃L³ = R-L-Asp [R = 3-hydroxy(5-hydroxymethyl)2-methylpyridine-4-methylene].

Table 8 Comparison of rate parameters for the formation of Al^{III} complexes with some related carboxylate ligands^a

Reacting species	$I/\text{mol dm}^{-3}$	$T/^\circ\text{C}$	$k_t/\text{dm}^3 \text{ mol}^{-1} \text{ s}^{-1}$	k_t/s^{1b}	Refs.
$\text{Al}^{3+} + [\text{Co}(\text{NH}_3)_5(\text{C}_2\text{O}_4)]^+$	1.0	30	2.47 ± 0.05	5.0×10^{-2}	9
$\text{AlOH}^{2+} + [\text{Co}(\text{NH}_3)_5(\text{C}_2\text{O}_4)]^+$	1.0	30	840	—	9
$\text{Al}^{3+} + [\text{Co}(\text{NH}_3)_5(\text{Hnta})]^+$	0.3	25	6.2×10^{-2}	—	This work
$\text{AlOH}^{2+} + [\text{Co}(\text{NH}_3)_5(\text{H}_2\text{nta})]^{2+}$	0.3	25	48	—	This work
$\text{AlOH}^{2+} + [\text{Co}(\text{NH}_3)_5(\text{Hnta})]^+$	0.3	25	85 ± 10	1.3×10^{-2}	This work
$\text{Al}^{3+} + [\text{Co}(\text{NH}_3)_5(\text{Hsal})]^{2+}$	0.1	30	0.16 ± 0.06	5.9×10^{-3}	41
$\text{AlOH}^{2+} + [\text{Co}(\text{NH}_3)_5(\text{Hsal})]^{2+}$	0.1	30	67 ± 15	—	41
$\text{Al}^{3+} + [\text{Co}(\text{NH}_3)_5(\text{Hnsal})]^{2+}$	0.1	30	0.10 ± 0.10	3.84×10^{-3}	41
$\text{AlOH}^{2+} + [\text{Co}(\text{NH}_3)_5(\text{Hnsal})]^{2+}$	0.1	30	8 ± 2	—	41
$\text{Al}^{3+} + \text{Hsal}^-$	0.1	30	0.78	—	42
$\text{AlOH}^{2+} + \text{Hsal}^-$	0.1	25	1.02×10^3	—	42

^a Hsal = Salicylic acid, Hnsal = 3-nitrosalicylic acid. ^b Spontaneous dissociation rate of Al^{III} complexes.

$k_{\text{ex}}(\text{FeOH}^{2+}) = 1.4 \times 10^5 \text{ s}^{-1}$, 25 °C^{37,40} suggests an associative (I_a) mechanism for Fe^{3+} (k_3 path) and an I_d mechanism for FeOH^{2+} (k_2 or k_4 paths). This is further supported by the fact that the activation parameters ΔH^\ddagger and ΔS^\ddagger (see Table 6) for the substitution reactions of Fe^{3+} and FeOH^{2+} are not substantially different from those for the water-exchange reaction of $[\text{Fe}(\text{OH}_2)_6]^{3+}$ ($\Delta H^\ddagger = 64 \text{ kJ mol}^{-1}$, $\Delta S^\ddagger = 12 \text{ J K}^{-1} \text{ mol}^{-1}$) and of $[\text{Fe}(\text{OH}_2)_5\text{OH}]^{2+}$ ($\Delta H^\ddagger = 42.4 \text{ kJ mol}^{-1}$, $\Delta S^\ddagger = 5.3 \text{ J K}^{-1} \text{ mol}^{-1}$).³⁷

For Al^{III} the plots of k_{obs} versus $[\text{Al}^{3+}]\{[\text{H}^+]/([\text{H}^+] + K_1)\}$ yielded [see equation (11)] k_f and k_r . The values of k_2 , k_3 and k_4 (see Table 5) were calculated by an identical procedure to that adopted for the Fe^{III} system. A comparison of the values of rate constants for the formation of Al^{III} complexes with some carboxylate ligands is given in Table 8. The magnitudes of the rate constants for the formation of $[(\text{NH}_3)_5\text{Co}(\text{nta})\text{Al}]^{3+}$ via the reaction of Al^{3+} or AlOH^{2+} with the nta cobalt(III) substrate are comparable to those obtained for the formation of $[(\text{NH}_3)_5\text{Co}(\text{sal})\text{Al}]^{4+}$ (ref. 41) but are lower than those for $[(\text{NH}_3)_5\text{Co}(\text{C}_2\text{O}_4)\text{Al}]^{4+}$.⁹ The values of k_3 (see Table 5) are smaller than the most recent data of water-exchange rate constant of $[\text{Al}(\text{OH}_2)_6]^{3+}$ ($k_{\text{ex}} = 16 \text{ s}^{-1}$ at 25 °C,⁴² $k_3/K_{\text{os}} =$

1.2 s^{-1} using $K_{\text{os}} = 0.05 \text{ dm}^3 \text{ mol}^{-1}$). The fact that $k_1 < k_{\text{ex}}$ eliminates the simple associative mechanism and supports an I_d mechanism. Similar conclusions were drawn previously for the complexation of Al^{III} with a number of co-ordinated carboxylate systems.⁴³ Much faster substitution reactions for $[\text{Al}(\text{OH}_2)_5\text{OH}]^{2+}$, as observed in the present work, are consistent with an I_d mechanism.

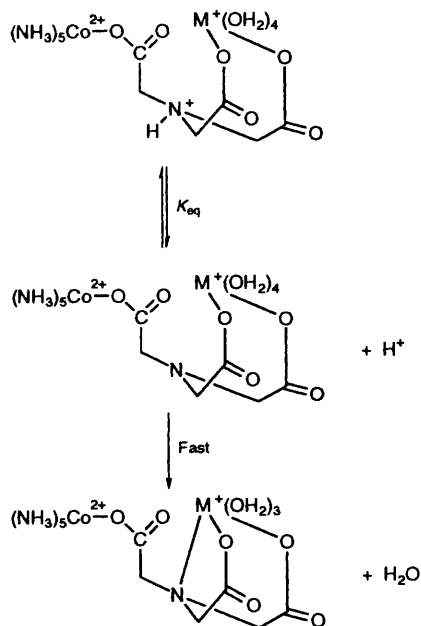
The binuclear species $[(\text{NH}_3)_5\text{Co}(\text{nta})\text{Al}]^{3+}$ undergoes spontaneous dissociation at a rate comparable with that of $[(\text{NH}_3)_5\text{Co}(\text{sal})\text{Al}]^{4+}$ or $[(\text{NH}_3)_5\text{Co}(\text{C}_2\text{O}_4)\text{Al}]^{4+}$ (see Table 8). Since Al^{3+} is chelated by the bound salicylate and oxalate moieties, it is presumed that the nta moiety chelates the metal ion in at least a tridentate mode. However, complexation of $[\text{Co}(\text{NH}_3)_5(\text{H}_2\text{nta})]^{2+}$ with trivalent metal ions, in contrast to that for bivalent metals, does not involve chelate-ring closure as the rate limiting step (step 2, Scheme 5). A similar conclusion was also drawn by Mentasti³⁸ for free-ligand complexation reactions.

The rate data for the acid-catalysed dissociation of $[(\text{NH}_3)_5\text{Co}(\text{nta})\text{Fe}]^{3+}$ are available as supplementary data. The observed rate constants were corrected for the formation reaction utilising the values ($k_2K_h + k_3K_1$), $k_4K_hK_1$ and $[\text{H}^+]$.

Table 9 Comparison of rate and activation parameters for the dissociation of some Fe^{III} complexes at 25 °C, *I* = 1.0 mol dm⁻³^a

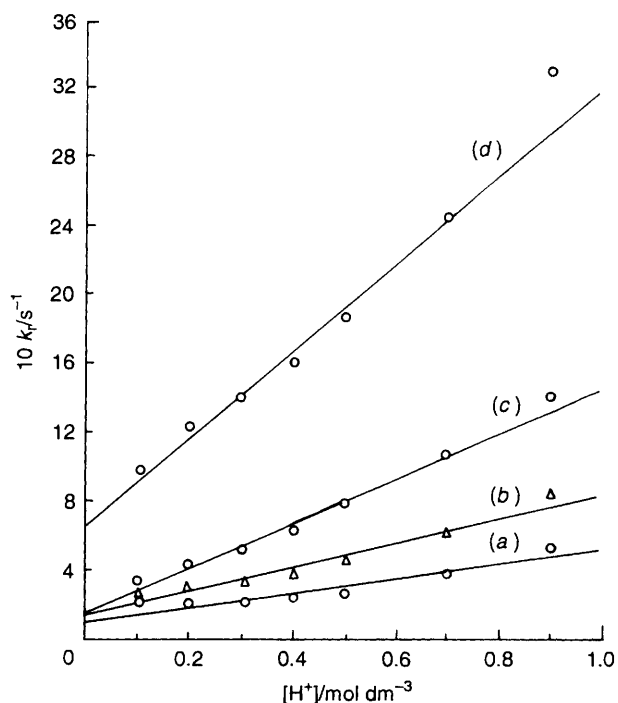
Fe ^{III} complex	k_s^b/s^{-1}	$\Delta H^\ddagger/kJ mol^{-1}$	$\Delta S^\ddagger/J K^{-1} mol^{-1}$	$k_a^b/dm^3 mol^{-1} s^{-1}$	$\Delta H^\ddagger/kJ mol^{-1}$	$\Delta S^\ddagger/J K^{-1} mol^{-1}$	Refs.
$[(NH_3)_5Co(sal)Fe]^{4+}$	0.23	63 ± 6	-50 ± 17	0.05	72 ± 12	-29 ± 38	3
<i>cis</i> - $[(en)_2(NH_3)Co(sal)Fe]^{4+}$	0.30	63 ± 2	-46 ± 8	0.09	64 ± 10	-50 ± 34	3
$\alpha\beta S$ - $[(tetren)Co(sal)Fe]^{4+}$	0.72	62 ± 2	-42 ± 8	0.29	70 ± 4	-21 ± 13	3
$[(NH_3)_5Co(C_2O_4)Fe]^{4+}$	negligible	—	—	0.50	44 ± 3	-99 ± 8	2
$[(NH_3)_5Co(nta)Fe]^{3+}$	0.24	61 ± 4	-31 ± 13	0.66	64 ± 4	-28 ± 14	This work
$[(NH_3)_5Co(mal)Fe]^{4+}$	5.11	—	—	—	—	—	6
$[Fe(pydca)]^+$	—	—	—	0.25	—	—	34
$[Fe(O_2CCH_2Cl)]^{2+}$	20	—	—	—	—	—	32

^a en = Ethylenediamine, tetren = tetraethylenepentamine. ^b k_s and k_a represent the spontaneous and acid-catalysed rate constants, respectively.

**Scheme 5** $M^{3+} = Fe^{3+}$ or Al^{3+}

The linear dependance of $k_r (= k_{obs} - k_r[M^{3+}])$ with $[H^+]$ (see Fig. 4) suggests that the last term in equation (7) is insignificant and can be neglected. The values of k_{-4} and $(k_{-2} + k_{-3})$ derived from the intercepts and slopes, respectively are also available as supplementary data. A comparison of rate and activation parameters for the dissociation of analogous Fe^{III} complexes are given in Table 9. The rate constant for the spontaneous dissociation, $k_4 (= k_s$ in Table 9) at all temperatures compares satisfactorily with the value of $k_r(av.)$ obtained from the formation study. It is also evident from Table 9 that the value of k_s for the nta complex is comparable with that obtained for $[(NH_3)_5Co(sal)Fe]^{4+}$ but significantly lower than that of $[Fe(O_2CCH_2Cl)]^{2+}$.³⁸ The relatively slow dissociation rate of the binuclear species may be taken as evidence that the Fe^{III} ion in $[(NH_3)_5Co(nta)Fe]^{3+}$ is chelated by the nta moiety in at least a tridentate co-ordination mode (see Scheme 5). A similar conclusion was reached by Cannon and Gardiner¹ in the study of Fe^{III}-catalysed aquation of $[Co(NH_3)_5(H_2nta)]^{2+}$. The rate and activation parameters for the acid-catalysed dissociation of $[(NH_3)_5Co(nta)Fe]^{3+}$ are also comparable with the values reported for related binuclear species (see Table 9). The activation parameters also fall in the range of ΔH^\ddagger (= 38–63 kJ mol⁻¹) and ΔS^\ddagger (= -42 to -126 J K⁻¹ mol⁻¹) values reported⁴⁴ for the dissociation of a series of $[FeL]^n+$ (L = F⁻, N₃⁻, Cl⁻, SCN⁻ or SO₄⁻) complexes.

In conclusion, the difference in the rate-determining steps for the complexation of bivalent and trivalent metal ions with

**Fig. 4** Plots of $k_r (= k_{obs} - k_r[Fe^{3+}])$ versus $[H^+]$ for the acid-catalysed dissociation of $[(NH_3)_5Co(nta)Fe]^{3+}$ at 15 (a), 20 (b), 25 (c) and 35 °C (d)

$[Co(NH_3)_5(H_2nta)]^{2+}$ may be explained as follows. The relatively greater coulombic repulsion between the NH^+ centre and the carboxylate-bound M^{3+} ion (as compared to M^{2+}) or favourable acid–base reaction of MOH^{2+} with the NH^+ site may result in the enhanced rate of proton transfer from the NH^+ centre of the binuclear species intermediate for M^{3+} ions [see Scheme 5 and equation (5)]. This may be responsible for proton transfer being equilibrium controlled for M^{3+} ions, while it is rate controlling for the M^{2+} ions (see Schemes 3 and 5). Accordingly general base catalysis was observed only for the complexation of the M^{2+} ions.

Acknowledgements

A. C. D. is thankful to Department of Science and Technology, New Delhi for financial support to purchase a stopped flow spectrophotometer and R. D. is thankful for the award of a Junior Research Fellowship.

References

- 1 R. D. Cannon and J. Gardiner, *Inorg. Chem.*, 1974, **13**, 390.
- 2 A. C. Dash and G. M. Harris, *Inorg. Chem.*, 1982, **21**, 1265.

- 3 A. C. Dash and G. M. Harris, *Inorg. Chem.*, 1982, **21**, 2336.
- 4 A. C. Dash, R. K. Nanda and A. N. Acharya, *Indian J. Chem., Sect. A*, 1991, **30**, 769.
- 5 A. C. Dash and J. Pradhan, *Int. J. Chem. Kinet.*, 1992, **24**, 155.
- 6 N. N. Das and R. K. Nanda, *Indian J. Chem., Sect. A*, 1991, **30**, 125.
- 7 A. C. Dash, R. K. Nanda and A. N. Acharya, *J. Chem. Soc., Dalton Trans.*, 1993, 1023.
- 8 R. Das and N. N. Das, *Transition Met. Chem.*, in the press.
- 9 P. Mohanty and A. C. Dash, *Transition Met. Chem.*, 1995, **20**, 153.
- 10 D. H. Bush and J. C. Bailar, jun., *J. Am. Chem. Soc.*, 1953, **75**, 4574.
- 11 A. C. Dash and R. K. Nanda, *Inorg. Chem.*, 1974, **13**, 655.
- 12 H. M. Irving and H. S. Rossotti, *J. Chem. Soc.*, 1954, 2904.
- 13 R. G. Wilkins, *Kinetics and Mechanism of Reactions of Transition Metal Complexes*, 2nd edn., VCH, New York, 1991, pp. 202, Table 4.1.
- 14 Y. Ducommun, K. E. Newman and A. E. Merbach, *Inorg. Chem.*, 1980, **19**, 3697.
- 15 Y. Ducommun, W. L. Carl and A. E. Merbach, *Inorg. Chem.*, 1979, **18**, 2754.
- 16 A. E. Merbach, *Pure Appl. Chem.*, 1987, **59**, 161.
- 17 R. B. Jordan, *Reaction Mechanism of Inorganic and Organometallic Systems*, Oxford University Press, Oxford, 1991.
- 18 D. H. Powell, L. Helm and A. E. Merbach, *J. Chem. Phys.*, 1991, **95**, 9258.
- 19 R. M. Fuoss, *J. Am. Chem. Soc.*, 1958, **80**, 5059.
- 20 T. J. Bydalek and M. L. Blomster, *Inorg. Chem.*, 1964, **3**, 667.
- 21 N. Tanaka and M. Kimura, *Bull. Chem. Soc. Jpn.*, 1967, **40**, 2100.
- 22 N. Tanaka and M. Kimura, *Bull. Chem. Soc. Jpn.*, 1968, **41**, 2375.
- 23 J. Maguire, *Can. J. Chem.*, 1974, **52**, 4106.
- 24 D. L. Rabenstein, *J. Am. Chem. Soc.*, 1971, **93**, 2869.
- 25 J. C. Cassatt and R. G. Wilkins, *J. Am. Chem. Soc.*, 1968, **90**, 6045.
- 26 D. B. Rorabacher, T. S. Turan, J. Defever and W. G. Nickels, *Inorg. Chem.*, 1969, **8**, 1498.
- 27 R. M. Milburn, *J. Am. Chem. Soc.*, 1957, **79**, 537.
- 28 R. K. Schofield and A. W. Taylor, *J. Chem. Soc.*, 1954, 4445.
- 29 E. Mentasti, E. Pelizzetti and G. Saini, *Gazz. Chim. Ital.*, 1974, **104**, 201.
- 30 S. Funahashi, A. Adachi and M. Tanaka, *Bull. Chem. Soc. Jpn.*, 1973, **46**, 479.
- 31 R. N. Pandey and N. W. Smith, *Can. J. Chem.*, 1972, **50**, 194.
- 32 B. Perlmutter-Hayman and E. Tapuhi, *J. Coord. Chem.*, 1976, **6**, 31.
- 33 E. G. Moohead and N. Sutin, *Inorg. Chem.*, 1966, **5**, 1866.
- 34 K. Bridger, R. C. Patel and E. Matijevic, *Polyhedron*, 1982, **1**, 269.
- 35 T. Ozawa, K. Jitsukawa, H. Masuda and H. Einaga, *Ber. Bunsenges. Phys. Chem.*, 1994, **98**, 66.
- 36 M. Eigen and R. G. Wilkins, *Adv. Chem. Ser.*, 1965, **49**, 55.
- 37 M. Grant and R. B. Jordan, *Inorg. Chem.*, 1981, **20**, 51.
- 38 E. Mentasti, *Inorg. Chem.*, 1979, **18**, 1512.
- 39 K. Ishihara, S. Funahashi and M. Tanaka, *Inorg. Chem.*, 1983, **22**, 194.
- 40 H. W. Dodgen, G. Liu and J. P. Hunt, *Inorg. Chem.*, 1981, **20**, 1002.
- 41 A. C. Dash, *Inorg. Chem.*, 1983, **22**, 837.
- 42 F. Secco and M. Venturini, *Inorg. Chem.*, 1975, **14**, 1978.
- 43 D. W. Margerum, G. R. Cayley, D. C. Weatherburn and G. K. Pagenkopf, *ACS Monogr.*, 1978, **174(2)**, 5.
- 44 F. P. Cavalasino, *J. Phys. Chem.*, 1968, **72**, 1378.

Received 3rd April 1995; Paper 5/02110C